Mon. Not. R. Astron. Soc. **000**, 000-000 (1999) Printed 4 April 2018 (MN plain TEX macros v1.6)

Radiation force on relativistic jets in active galactic nuclei

Qinghuan Luo and R. J. Protheroe

Department of Physics and Mathematical Physics, The University of Adelaide, Adelaide, SA 5005, Australia

Accepted date; Received date

ABSTRACT

Radiative deceleration of relativistic jets in active galactic nuclei as the result of inverse Compton scattering of soft photons from accretion discs is discussed. The Klein-Nishina (KN) cross section is used in the calculation of the radiation force due to inverse Compton scattering. Our result shows that deceleration due to scattering in the KN regime is important only for jets starting with a bulk Lorentz factor larger than 10^3. When the bulk Lorentz factor satisfies this condition, particles scattering in the Thomson regime contribute positively to the radiation force (acceleration), but those particles scattering in the KN regime are dominant and the overall effect is deceleration. In the KN limit, the drag due to Compton scattering, though less severe than in the Thomson limit, strongly constrains the bulk Lorentz factor. Most of the power from the deceleration goes into radiation and hence the ability of the jet to transport significant power (in particle kinetic energy) out of the subparsec region is severely limited. The deceleration efficiency decreases significantly if the jet contains protons and the proton to electron number density ratio satisfies the condition $n_p/n_{e0} > 2\gamma_{\rm min}/\mu_p$ where $\gamma_{\rm min}$ is the minimum Lorentz factor of relativistic electrons (or positrons) in the jet frame and μ_p is the proton to electron mass ratio.

Key words: Scattering – plasmas – relativistic jets – AGN – radiation: nonthermal

1 INTRODUCTION

High energy observations of blazars strongly suggest that the emission comes from relativistic jets of active galactic nuclei (AGN) (e.g. von Montigny et al. 1995; Thompson et al. 1995; Gaidos et al. 1996; Quinn et al. 1996; Schubnell et al. 1996). Other evidence for relativistic AGN jets includes the observation of variability in radio, optical, and high energy gamma ray emission from blazars. Although there is no consensus on the details of AGN, it is widely accepted that a jet may form near a black hole with an accretion disc (e.g. a review by Blandford 1990). Since a substantial fraction of the binding energy of accreting material is dissipated and converted to radiation, the disc is a strong source of soft photons (e.g. as black body radiation or reprocessed radiation). Interaction of relativistic particles in the jet with these surrounding photon fields can be important, and may contribute to the observed gamma ray emission, e.g. through inverse Compton scattering (Reynolds 1982; Melia & Königl 1989; Dermer & Schlickeiser 1993). Disk emission can also affect the jet dynamics near the black hole through radiative acceleration or deceleration. The effect of Compton scattering on the jet flow was discussed by O'Dell (1981), and Phinney (1982, 1987), and it was suggested that under certain (quite stringent) conditions, the jet can be accelerated through Compton scattering. However, as pointed out by several authors (e.g. Phinney 1987; Melia & Königl 1989; Sikora et al. 1996), in the region close to the black hole, Compton scattering can be more effective in slowing down rather than accelerating the jet, and can constrain the bulk flow of the jet in that region.

There are AGN emission models in which protons are accelerated to ultra high energies (e.g. Königl 1994). One of the attractive features of this type of model is that protons can be accelerated to high energies without significant energy loss. These high energy protons can interact with photon fields producing electron-positron pairs. It is possible that through pair cascades, an ultrarelativistic jet is produced. Alternatively, an ultrarelativistic jet can be produced through rapid acceleration of $e^{\pm}$ such as by magnetic reconnection (e.g. Haswell et al. 1992) or by rotation-induced electrostatic potential drop as in pulsars (Michel 1987). In both cases, the bulk flow of the jet may initially have a large Lorentz factor, and plasmas in the jet can be highly relativistic. Therefore, scattering in the Klein-Nishina (KN) regime is important, and should be included in calculation of radiation force due to inverse Compton scattering. There is then the question of whether the jet with initially large bulk flow speed is subject to the same (severe) radiation deceleration as in the Thomson regime, and this will be explored in this paper.

The constraint on the bulk flow by Compton scattering should strongly depend on the soft photon distribution of the disc. In our discussion, disc emission is assumed to be axisymmetric, and so the only effect on the jet flow considered is in the jet direction (it is usually assumed that the jet is normal to the disc plane). However, there are cases in which accretion may not be circular, e.g. eccentric accretion can occur if the black hole is in a binary system (e.g. Begelman, Blandford & Rees 1980; Eracleous et al. 1995), and this possibility will be considered in a forthcoming paper (Luo 1998).

The deceleration efficiency strongly depends on the composition of the jet. An AGN jet that contains protons would be subject to less severe deceleration because protons scatter photons with much smaller cross section than that for electrons (or positrons) and this effectively increases the jet inertia.

In this paper, we extend calculations of the radiation force by including the Klein-Nishina effect as the earlier calculations were done only in the Thomson scattering regime (e.g. O'Dell 1981; Phinney 1982; Sikora et al. 1996). In Sec. 2, the average radiation force on the bulk plasma flow is derived in both the Thomson and Klein-Nishina limits. Constraints by radiative deceleration on the Lorentz factor of the jet are discussed in Sec. 3.

2 RADIATIVE EFFECT ON JET FLOW

Through Compton scattering of external photons, individual particles in plasmas lose energy and at the same time there is momemtum transfer to the plasma. For plasmas in a jet, the momemtum transfer can affect the jet dynamics, i.e. the bulk flow can be either accelerated or decelerated (i.e. radiative drag).

Consider a comoving cell with energy $\tilde{E}$ (in m_ec^2 per unit volume) in a relativistic jet with the bulk Lorentz factor $\Gamma = 1/(1-\beta_{\rm b}^2)^{1/2}$ where $\beta_{\rm b}$ is the bulk velocity in c. The tilded quantities correspond to the values in the lab frame (K). We assume that the jet contains mainly electron-positron pairs (there may be protons as well but in small number) and that within the cell electron-positron pair production is not important. The latter assumption may not be accurate since pairs can be injected continuously along the jet. Nonetheless, it allows us to single out the radiative effect due to Compton scattering, and the result should not change qualitatively when the pair production effect is included. Let f be the radiative force (in m_ec per second per unit volume) on the cell seen in the jet comoving frame (K_j). Then, the rate of change of Γ due to radiation force on the cell is given by (e.g. Phinney 1982; Sikora et al. 1996)

$$\frac{d\Gamma}{dt} = \frac{\beta_{\rm b} f_z}{E}, \tag{2.1}$$

where E is the cell energy in K_j, and we assume that the jet is along the z direction. Then, for $f_z > 0$, the jet is accelerated away from the source, and for $f_z < 0$, it is decelerated toward the source, i.e. radiation drag. In (2.1), the average force f_z depends on the particle distribution which is influenced by the specific acceleration or energy loss mechanisms. In the following discussion, we only consider radiative effects due to Compton scattering.

2.1 Radiation from the disc

To study the radiative effect on jet dynamics due to inverse Compton scattering, a specific model for the external photon field is required. We assume that the external photon field is the accretion disc emission, and is axisymmetric with respect to the jet axis (which is in the z direction). A schematic diagram for such a disc-jet system is shown in Figure 1. Emission from the disc is modeled as the sum of emission from series of rings centered at the black hole; each of them emits photons with a characteristic energy $\tilde{\varepsilon}_R$ where R is the radius of the ring. The flux number density of photons from the ring $R \sim R + dR$ is given by $F(\tilde{\varepsilon}, R) = F(R)\delta(\tilde{\varepsilon} - \tilde{\varepsilon}_R)$ where $\tilde{\varepsilon} = \Gamma(1+\beta_{\rm b}\cos\theta)\varepsilon$ is the photon energy (in m_ec^2) seen in K, ε is the corresponding energy seen in K_j, θ is the angle between the photon propagation direction and the jet axis, and $F(R)$ is given by (Blandford 1990)

$$\begin{aligned} F(R) \approx & 4.4\times 10^{30}\left(\frac{1\,{\rm eV}}{\tilde{\varepsilon}_R}\right)\left(\frac{\dot{M}}{L_{\rm Edd}/c^2}\right) \\ & \times\left(\frac{M}{10^8 M_\odot}\right)^{-1}\left(\frac{R}{GM/c^2}\right)^{-3} I\,{\rm cm}^{-2}\,{\rm s}^{-1}, \end{aligned} \tag{2.2}$$

where $I = (1 - R_{\rm min}/R)^{1/2}$, $R_{\rm min}$ is the radius of the innermost part of the disc, M is the mass of the black hole, G is Newton's constant, $L_{\rm Edd}$ is the Eddington luminosity. We assume $R_{\rm max}$ to be the maximum radius of the disc, within which emission can be adequately described by (2.2).

A detailed model for emission from the accretion disc should include effects such as reprocessing of radiation, disc corona, etc. As we are concerned with the radiative effect on the jet flow, all these details will be ignored and we assume that disc emission is blackbody with $\tilde{\varepsilon}_R \approx 2.7k_{\rm B}T(R)/m_ec^2$, where $T(R)$ is the effective temperature of emission from the ring with R. Then, for an optically thick disc, $T(R)$ is identified as the surface temperature, and it is given by $T(R) = (3GM\dot{M}I/8\pi R^3\sigma_{\rm SB})^{1/4}$, that is,

$$\begin{aligned} T(R) \approx & 5\times 10^5\left(\frac{\dot{M}}{L_{\rm Edd}/c^2}\right)^{1/4}\left(\frac{M}{10^8 M_\odot}\right)^{-1/4} \\ & \times\left(\frac{R}{GM/c^2}\right)^{-3/4} I^{1/4}\,{\rm K}, \end{aligned} \tag{2.3}$$

where $R \geq R_{\rm min}$, $\sigma_{\rm SB}$ is the Stefan-Boltzmann constant. Figure 2 shows plots of $F(R)$ for $R_{\rm min}/R_g = 5$ and 6, where $R_g = GM/c^2 \approx 1.48\times 10^{13}\,{\rm cm}\,(M/10^8\,M_\odot)$ is the gravitational radius. The fluxes are peaked at $R_0 = (7/6)R_{\rm min} \approx 5.8R_g$ and $7R_g$, respectively.

Let $n_{\rm ph}(\varepsilon, \Omega, R)dR$ be the number density of photons emitted from the ring between R and $R + dR$, where ε and $\Omega = (\phi, \cos\theta)$ are the energy and direction of incoming photons, respectively. Using (2.2), the photon number density (per unit R), $n_{\rm ph}(\varepsilon, \Omega, R)$, in K_j can be written as (e.g. Dermer & Schlickeiser 1993)

$$n_{\rm ph}(\varepsilon, \Omega, R) = \frac{RF(\tilde{\varepsilon}, R)}{2\pi c(R^2+z^2)}\,\delta\!\left(\cos\theta - \frac{\cos\tilde{\theta}_R - \beta_{\rm b}}{1-\beta_{\rm b}\cos\tilde{\theta}_R}\right), \tag{2.4}$$

where $\cos\tilde{\theta}_R = z/(R^2+z^2)^{1/2}$, z is the distance from the disc surface, $\tilde{\theta}_R$ is the angle of incoming photons relative to the the jet axis in K_j.

2.2 Radiation force

The radiation force f (on the jet bulk flow) can be derived by calculating the rate of average momemtum transfer to

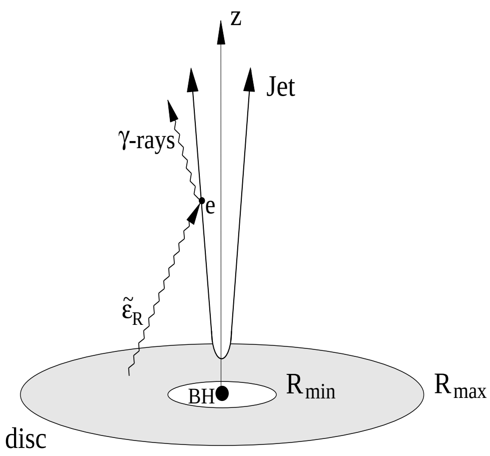

Figure 1. A schematic diagram of an AGN jet.

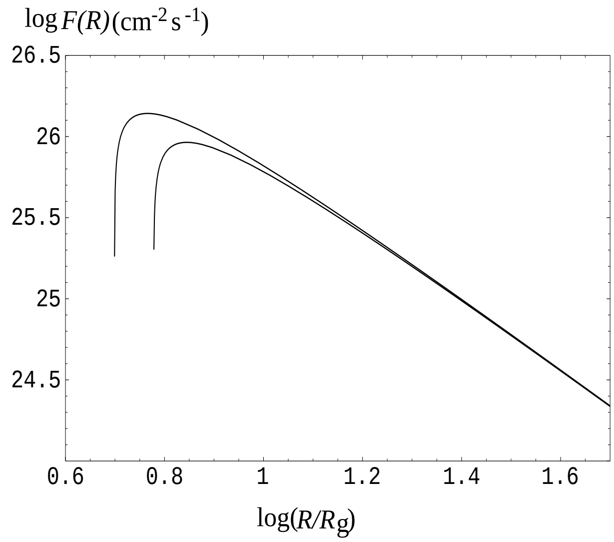

Figure 2. Photon flux density from the ring as a function of R. We assume $M = 10^8 M_\odot$, $\dot{M} = 0.1 L_{\rm Edd}/c^2$. The upper and lower curves are obtained by assuming $R_{\rm min} = 5R_g$ and $6R_g$, respectively.

plasmas in the jet as a result of inverse Compton scattering, which is given by

$$\begin{aligned}\mathbf{f} &= \int d\Omega_e d\gamma \, \frac{d\mathbf{p}}{dt} \, n_e(\gamma, \Omega_e) \\ &= -c \int dR \int d\Omega_e d\gamma \, n_e(\gamma, \Omega_e) \int d\varepsilon \int d\Omega \, n_{\rm ph}(\varepsilon, \Omega, R) \, D \\ &\times \int d\varepsilon_s \int d\Omega_s \left(\frac{d\sigma}{d\varepsilon_s d\Omega_s} \right) (\varepsilon_s \hat{\mathbf{k}}_s - \varepsilon \hat{\mathbf{k}}),\end{aligned} \tag{2.5}$$

where $D = 1 - \beta \cdot \hat{\mathbf{k}}$, $\gamma = 1/(1-\beta^2)^{1/2}$ is the particle Lorentz factor in the jet frame (K_j), $n_{\rm ph}(\varepsilon, \Omega)$ is the photon density, $\mathbf{p} = \gamma\beta$ is the momemtum (in $m_e c$), $n_e(\gamma, \Omega_e)$ is the particle distribution, $\Omega_e = (\phi_e, \cos\theta_e)$ is the direction of electron motion, $d\sigma/d\varepsilon_s d\Omega_s$ is the differential cross in K_j whose approximations in the Thomson and KN regimes are given respectively by (A1) and (A2). The direction of incoming and scattered photons in K_j are represented by $\hat{\mathbf{k}}$ and $\hat{\mathbf{k}}_s$, respectively. All quantities with subscript s are for scattered photons. As we use axisymmetric disk emission as given by (2.2), the only relevant component of the force is along z axis.

We first derive the radiation force in the Thomson limit. In the Thomson scattering regime, scattering is elastic and we have $\varepsilon'_s \approx \varepsilon'$ where ε' and ε'_s are respectively the energies of the incoming and scattered photon in the electron rest frame (K'). Further, we assume a beaming approximation in which the scattered photons propagate approximately in the electron's direction in K_j provided that $\gamma \gg 1$. Based on these considerations, an approximation for the differential cross section in K_j can be obtained as (A1), and the force is calculated as

$$\begin{aligned}f_z =& \sigma_{\rm T} \int_{R_{\rm min}}^{R_{\rm max}} dR \, \frac{R\, F(R)}{R^2 + z^2} \, \Gamma^2 \tilde{\varepsilon}_R (1 - \beta_{\rm b} \cos\tilde{\theta}_R) \\ & \times (\cos\tilde{\theta}_R - \beta_{\rm b}) \left(\tfrac{2}{3} \langle \gamma^2 \beta \rangle + 1 \right) n_{e0},\end{aligned} \tag{2.6}$$

where we assume that the disc emission is important within $R_{\rm min} \le R \le R_{\rm max}$, σ_T is the Thomson cross section, the average is made over the electron (or positron) distribution, $\langle ... \rangle = \int d\Omega_e d\gamma \, (...) n_e(\gamma, \Omega_e)/n_{e0}$, and n_{e0} is the average number density. The distribution $n_e(\gamma, \Omega_e)$ is assumed to be isotropic in K_j with a power law:

$$n_e(\gamma, \Omega_e) = \frac{C_0}{4\pi} n_{e0} \gamma^{-p}, \tag{2.7}$$

where p is the electron spectral index with values between 2 and 3, $\gamma_{\rm min} \le \gamma \le \gamma_{\rm max}$, the constant C_0 is chosen such that (2.7) is normalized to n_{e0}. We assume the cyclotron time scale is much less than the relevant time scales of acceleration or deceleration, electron (positron) energy loss. Therefore, all quantities in (2.7) can be regarded as average over the cyclotron time. For $\gamma_{\rm max} \gg \gamma_{\rm min}$ and $p \ge 2$, we have $C_0 \approx (p-1)\gamma_{\rm min}^{p-1}$. Using (2.7), we have $\langle \gamma^2 \rangle \approx [(p-1)/(3-p)] \gamma_{\rm min}^{p-1} (\gamma_{\rm max}^{3-p} - \gamma_{\rm min}^{3-p})$ which reduces to $\langle \gamma^2 \rangle \approx 2\gamma_{\rm min}^2 \ln(\gamma_{\rm max}/\gamma_{\rm min})$ for $p = 3$.

It follows from (2.6) that acceleration ($f_z > 0$) occurs for $\cos\tilde{\theta}_R > \beta_{\rm b}$ corresponding to when electrons see most incoming photons with $\theta_R \approx 0$, and deceleration ($f_z < 0$) for $\cos\tilde{\theta}_R < \beta_{\rm b}$ corresponding to when electrons see most photons with $\theta_R \approx \pi$ in the jet frame. Therefore, the key role in radiative acceleration or deceleration is played by anisotropic scattering, which can be understood as follows. Assume a cell moving along the jet containing relativistic plasma with an isotropic distribution. The particles in the jet frame see anisotropic photon fields, i.e. the radiation mainly comes from behind or in front depending on Γ of the bulk motion. When $\cos\tilde{\theta}_R < \beta_{\rm b}$, in the jet frame, although each electron would scatter photons into its direction of motion, on average there is more momemtum beamed along the jet direction. Thus, the cell is subject to a force in the opposite direction. The critical Γ, above which the radiative deceleration ($f_z < 0$) occurs, can be derived from (2.6) by setting $f_z = 0$ (e.g. Sikora et al. 1996). Since the critical Γ is generally small (e.g. Phiney 1987; Sikora et al. 1996), our discussion concentrates on deceleration of jets with a large initial Γ.

In the case of deceleration, since the flux (2.2) is peaked at $R = R_0 = (9/7)R_{\rm min}$, an approximation for f_z at $z \gg R_0$

is given by

$$f_z \approx -\tfrac{1}{3}\mu_p \eta \Gamma^2 \frac{R_g c}{z^2}\left(\frac{R_0}{z}\right)^4 \langle\gamma^2\rangle n_{e0}$$
$$= -\tfrac{2}{3}\mu_p \eta \Gamma^2 \frac{R_g c}{z^2}\left(\frac{R_0}{z}\right)^4 \gamma_{\min}^2 n_{e0}\, \ln(\gamma_{\max}/\gamma_{\min}), \qquad (2.8)$$

where $\mu_p = m_p/m_e$ is the proton to electron mass ratio, $R_0 = 7R_{\min}/6$ is the radius at which the flux is peaked, $\eta = L_d/L_{\rm Edd}$ is the radiation efficiency of disc emission, $L_{\rm d} = 2\pi m_e c^2 \int dR\, RF(R)\tilde{\varepsilon}_R$ is the luminosity of the source, and the equality is for $p = 3$. The radiation force increases rapidly with Γ^2.

Although (2.6) is derived using the beaming approximation as described by $\delta(\Omega_s - \Omega_e)$ in Eq. (A1), apart from $\beta \approx 1$ in the average $\langle\gamma^2\beta\rangle$, it is in good agreement with the result derived by Sikora et al. (1996) using covariant formalism. One may also reproduce the result given by O'Dell (1981) where the photons are from a point source, for which we may assume $\tilde{\theta}_R = 0$ and that $2\pi \int dR\, RF(R)\tilde{\varepsilon}_R \to L_{\rm d}/m_e c^2$ is the luminosity of the source. In this special case, the particles are accelerated away from the source.

In calculating (2.6) and (2.8), we assume $\varepsilon' < 1$. In the electron rest frame, the photon energy is $\varepsilon' = \varepsilon'_R \equiv \gamma(1 - \beta\cos\Theta_R)\Gamma(1 - \beta_b \cos\tilde{\theta}_R)\tilde{\varepsilon}_R$, where Θ_R is the angle between the incoming photon direction and electron motion (in K_j). Then, the condition for *all* particles to scatter in the Thomson regime is

$$\gamma\varepsilon_R < 1/2. \qquad (2.9)$$

with $\varepsilon_R = \Gamma(1 - \beta_b\cos\tilde{\theta}_R)\tilde{\varepsilon}_R$. This condition requires that photons of the highest energy, seen by particles with $\Theta_R = \pi$, satisfy $\varepsilon'_R < 1$, which may not be the case if Γ, or the average Lorentz factor ($\langle\gamma\rangle$) of the plasma in K_j, are large.

2.3 The Klein-Nishina regime

For an ultrarelativistic jet with a large bulk Lorentz factor or when particles are highly relativistic in the jet comoving frame, Compton scattering should be treated in the Klein-Nishina scattering regime. The minimum Γ such that *all* particles of energy γ are in the KN regime can be derived as follows. In the jet frame, since the soft photon direction is $\theta_R \approx \pi$, electrons with $\theta_e = \pi$ see the lowest energy photons. Since $\cos\Theta_R = \cos\theta_R\cos\theta_e + \sin\theta_R\sin\theta_e\cos(\phi - \phi_e) \approx -\cos\theta_R\cos\theta_e$ (where ϕ and ϕ_e are the azimuthal angles of the photon and electron), and from $\varepsilon'_R \geq 1$, we can derive the condition for all particles to scatter in the KN regime,

$$\frac{\Gamma}{\gamma} > \frac{2}{\tilde{\varepsilon}_R(1 - \beta_b\cos\tilde{\theta}_R)}, \qquad (2.10)$$

or

$$\frac{\Gamma}{\gamma} < \tfrac{1}{2}\tilde{\varepsilon}_R(1 + \cos\tilde{\theta}_R), \qquad (2.11)$$

where we assume that the plasma is relativistic in the jet frame. For $\tilde{\varepsilon}_R = 6 \times 10^{-5}$, we have $\Gamma/\gamma > 5 \times 10^4/(1 - \cos\tilde{\theta}_R)$ or $\Gamma/\gamma < 3 \times 10^{-5}(1 + \cos\tilde{\theta}_R)$. Inequalities (2.10) and (2.11) are the KN condition for particles of γ with any θ_e, which requires an extreme ratio (very large or very small) Γ/γ. However, in the following discussion we show that the condition for the KN scattering to be the dominant process

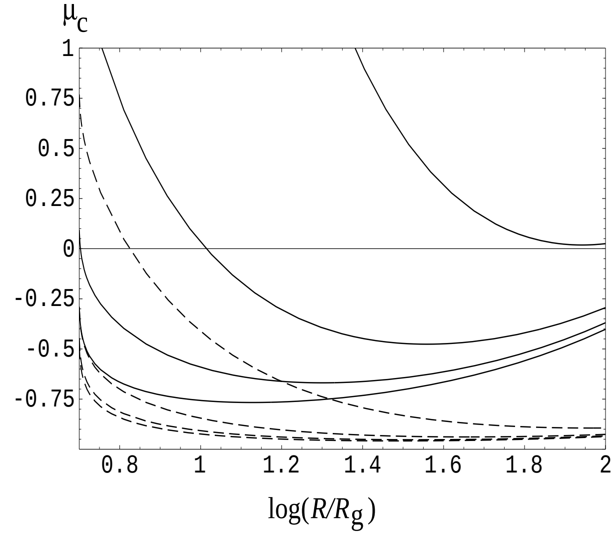

Figure 3. Plots μ_c as a function of R/R_g for different z and γ. The solid and dashed curves correspond respectively to $\gamma = 10^2$ and 10^3. In each case, the curves from bottom to top correspond to $z/R_g = 5, 10, 30, 50$. We assume the bulk Lorentz factor $\Gamma = 10^4$.

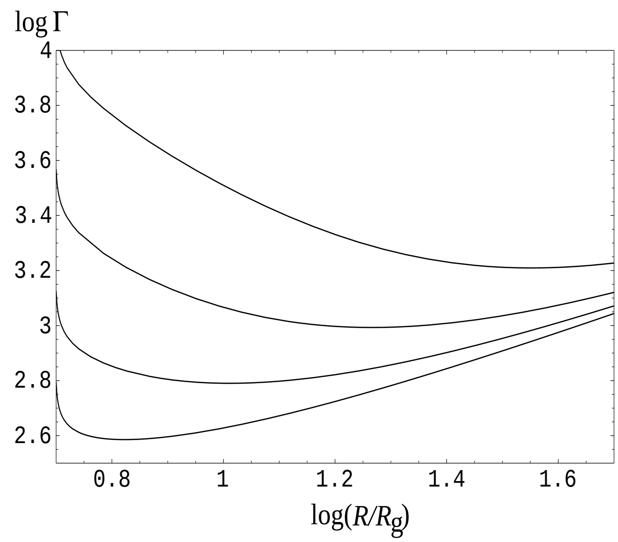

Figure 4. The minimum Γ for KN scattering to be dominant in deceleration are plotted as functions of R/R_g. The curves from top to bottom correspond to $z/R_g = 20, 10, 5, 2$. We assume $\gamma_{\min} = 80$, $R_{\min} = 5R_g$, and use the temperature function (2.3) with $\dot{M} = 0.1L_{\rm Edd}/c^2$.

in radiative drag is less strict than (2.10), (2.11), and is generally satisfied for moderate Γ.

In general, given a particle distribution, the Thomson and KN approximations apply respectively to particles with $\cos\theta_e < \mu_c$ and $\cos\theta_e \geq \mu_c$, where μ_c satisfies $\Gamma\gamma(1 - \beta\mu_c\cos\theta_R)(1 - \beta_b\cos\tilde{\theta}_R)\tilde{\varepsilon}_R = 1$, that is,

$$\mu_c = \begin{cases} \dfrac{1}{\beta}\,\dfrac{1 - \Gamma\gamma(1 - \beta_b\cos\tilde{\theta}_R)\tilde{\varepsilon}_R}{\Gamma\gamma(\beta_b - \cos\tilde{\theta}_R)\tilde{\varepsilon}_R}, & \text{for } \gamma\varepsilon_R \geq 1/2; \\ 1, & \text{for } \gamma\varepsilon_R < 1/2. \end{cases} \qquad (2.12)$$

Thus, the conditions (2.10), (2.11) correspond to an extreme case; if one of these two conditions is satisfied, then $\mu_c = -1$, and in this case the KN approximation applies to *all* particles. Figure 3 shows plots of μ_c as functions of R/R_g. For given z and γ, the KN scattering regime is located above the curve (i.e. for electrons or positrons with $\cos\theta_e \ge \mu_c$).

To calculate f_z, particles of energy γ in the cell are divided into two parts according to (2.12). Let $f_{z,\rm T}$ and $f_{z,\rm KN}$ be the force due to scattering by particles with $\cos\theta_e \le \mu_c$ (the Thomson regime) and $\cos\theta_e > \mu_c$ (the KN regime), respectively. Then, the radiation force can be expressed as

$$f_z = f_{z,\rm T} + f_{z,\rm KN}. \tag{2.13}$$

where $f_{z,\rm T}$ and $f_{z,\rm KN}$ can be calculated approximately using the cross sections (A1), (A2) as given in the Appendix (cf. Eq. A4 and A5). Assuming that incident photons in the jet frame are approximately beamed, $\cos\theta_R \approx -1$, which is valid for $\Gamma \gg 1$, we have

$$\begin{aligned} f_{z,\rm T} = &-\tfrac{1}{2}\sigma_{\rm T} C_0 n_{e0}\int_{R_{\min}}^{R_{\max}} dR\,\frac{RF\tilde{\varepsilon}_R\Gamma^2}{2\pi(R^2+z^2)}(1-\beta_b\cos\tilde{\theta}_R)^2 \\ &\times\int_{\gamma_{\min}}^{\gamma_{\max}} d\gamma\,\gamma^{-p}\Big\{\gamma^2\Big[\tfrac{1}{2}(\mu_c^2-1)+\tfrac{2}{3}(\mu_c^3+1)+\tfrac{1}{4}(\mu_c^4-1)\Big] \\ &+(\mu_c+1)+\tfrac{1}{2}(\mu_c^2-1)\Big\}, \end{aligned} \tag{2.14}$$

and

$$\begin{aligned} f_{z,\rm KN} \approx &-\tfrac{3}{8}\sigma_{\rm T} C_0 n_{e0}\int_{R_{\min}}^{R_{\max}} dR\,\frac{RF}{2\pi(R^2+z^2)}\,\frac{1}{4\tilde{\varepsilon}_R} \\ &\times\int_{\gamma_{\min}}^{\gamma_{\max}} d\gamma\,\gamma^{-p}\Big\{\big(1-\mu_c^2\big)\ln 2+(1-\mu_c) \\ &+\frac{2\varepsilon_R}{\gamma}\Big[(1-\mu_c)\ln(2/\sqrt{e})+2\ln(2\varepsilon_R\gamma)\Big]\Big\}H(\gamma\varepsilon_R-\tfrac{1}{2}), \end{aligned} \tag{2.15}$$

where $H(\gamma\varepsilon_R-1/2)=1$ for $\gamma\varepsilon_R \ge 1/2$ and $H(\gamma\varepsilon_R-1/2)=0$ for $\gamma\varepsilon_R < 1/2$. In the Thomson approximation, $\mu_c = 1$, we have $f_z = f_{z,\rm T}$, which reduces to (2.6) with $\cos\theta_R \approx -1$. For $\mu_c < 1$, $f_{z,\rm T}$ can be positive even though we assume $\cos\theta_R = -1$. This is because $f_{z,\rm T}$ includes particles with $-1 \le \cos\theta_e < \mu_c$, and if most of them have $\theta_e > \pi/2$ we would have $f_{z,\rm T} > 0$. In contrast, $f_{z,\rm KN}$ is always negative since it includes only those particles with $\mu_c < \cos\theta_e \le 1$, most of which move forward along the jet and contribute to drag. From (2.14) and (2.15), we see that when $\mu_c < 1$ scattering in the KN regime becomes important while the force due to scattering in the Thomson regime starts to decrease. From (2.12), this condition becomes

$$\Gamma \ge \frac{1}{2\gamma(1-\beta_b\cos\tilde{\theta}_R)\tilde{\varepsilon}_R}. \tag{2.16}$$

Figure 4 shows the condition (2.16) as a function of R with γ being replaced by $\langle\gamma\rangle$. We assume $\gamma = 80$, $p = 3$. Thus, the average Lorentz factor in the jet frame is $\langle\gamma\rangle = 160$. This gives, for example, $\Gamma > 400$ for $z = 2R_g$, and $\Gamma > 700$ for $z = 5R_g$. These lower limits can be further reduced as scattering in the KN regime extends to higher γ.

Integration over γ in Eq. (2.14) and (2.15) can be done analytically using (2.7), and is given by Eq. (A8), (A9) in the Appendix. For $2\varepsilon_R < 1/\gamma_{\min}$, (2.15) has the following approximation

$$f_{z,\rm KN} \approx -\alpha\sigma_T n_{e0}\int_{R_{\min}}^{R_{\max}} dR\,\frac{RF(R)}{2\pi(R^2+z^2)}\,\frac{3(\varepsilon_R\gamma_{\min})^{p-1}}{16\tilde{\varepsilon}_R}, \tag{2.17}$$

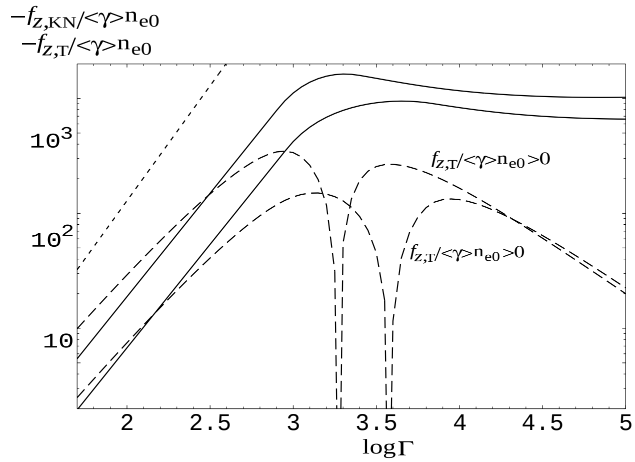

Figure 5. Variation of $f_{z,\rm T}/\langle\gamma\rangle n_{e0}$ (dashed), $f_{z,\rm KN}/\langle\gamma\rangle n_{e0}$ (solid) with Γ for $z = 5R_g$ (upper) and $z = 10R_g$ (lower). The dotted curve (for $z = 5R_g$) is calculated by ignoring scattering in the KN regime.

with $\alpha = 2/(p-1)+\ln(64e)/p-\ln 2/(p+1)$, which ranges from 4.4 ($p = 2$) to 2.6 ($p = 3$). For large Γ satisfying (2.16), $f_{z,\rm KN}$ overtakes $f_{z,\rm T}$ and become important. For even larger Γ, we find

$$\begin{aligned} f_z \approx f_{z,\rm KN} = &-\tfrac{3}{8}\sigma_{\rm T} n_{e0}\int_{R_1}^{R_{\max}} dR\,\frac{RF}{2\pi(R^2+z^2)} \\ &\times\frac{1}{2\tilde{\varepsilon}_R}\Big[1+\frac{2\varepsilon_R(p-1)}{\gamma_{\min}p}\ln(2\varepsilon_R\gamma_{\min})\Big], \end{aligned} \tag{2.18}$$

where R_1 is the radius of the ring which emits photons with energy $\varepsilon_R = 1/(2\gamma_{\min})$. If $\varepsilon_R > 1/(2\gamma_{\min})$ for $R_{\min} \le R \le R_{\max}$, R_1 is replaced by $R_{\min}$. Figure 5 shows $f_{z,\rm T}/\langle\gamma\rangle n_{e0}$ (Eq. 14), $f_{z,\rm KN}/\langle\gamma\rangle n_{e0}$ (Eq. 15) as functions of Γ for $z = 5R_g$, $10R_g$. The disc parameters are the same as in Figure 2. We assume $p = 2.8$, $R_{\min} = 5R_g$, $R_{\max} = 50R_g$. The value of f_z is significantly lower than that calculated using the Thomson approximation (dotted curve), indicating the importance of the KN scattering. The KN scattering starts to overtake the Thomson scattering when $\Gamma > 300$ for $z = 5R_g$ and $\Gamma > 200$ for $z = 10R_g$, and it is described by Eq. (2.17). Scattering in the KN regime becomes dominant in decelerating the jet at $\Gamma > 10^3$ and the approximation (2.18) applies. The force component due to scattering in the Thomson regime becomes positive for large Γ since most particles that scatter in the Thomson regime move toward the black hole and hence contribute to acceleration of the cell. However, the net force is still negative because the component due to forward moving particles that scatter in the KN regime dominates. For extremely large Γ, we may have $2\varepsilon_R > p\gamma_{\min}/(p-1)\ln(2\varepsilon_R\gamma_{\min})$, and then, the second term on the right hand side of (2.18) becomes important, and $f_z \approx f_{z,\rm KN}$ increases logarithmically with Γ.

3 RADIATIVE DECELERATION

A relativistic jet can form in the vicinity of a black hole through either (1) a hydrodynamic process, in which radiation from an accretion disc plays an important role in producing and collimating the jet, or (2) a MHD process, in which magnetic fields play major role in the jet flow. In either case, regardless of the details of jet production, which are poorly understood, the jet must pass through intense radiation fields from disc emission and be subject to radiative deceleration. In the following discussion, we assume that the jet has initially a large Γ and then undergoes deceleration due to the radiation force discussed in earlier sections, and we examine the constraint on the bulk flow when scattering in the KN regime is included.

3.1 Constraint on Γ

The bulk Lorentz factor Γ as a function of z can be calculated by integrating (2.1) along the jet direction. For deceleration from the KN to Thomson regime, we use (2.13) together with (2.14) and (2.15) for which integration over R can be done numerically. We first consider an electron positron jet with an energy density (in $m_e c$) given by $E = n_{e0}\langle\gamma\rangle$. (A relativistic jet containing protons will be considered in Sec.3.2.) From the distribution (2.7), we have

$$E \approx n_{e0}\gamma_{\min}\frac{p-1}{p-2}\left[1-\left(\frac{\gamma_{\min}}{\gamma_{\max}}\right)^{p-2}\right], \tag{3.1}$$

for $p > 2$ and $\gamma_{\max} \gg \gamma_{\min}$. Figure 6 shows $d\ln\Gamma/dz$ as a function of z and γ. Radiative drag is severe, i.e. $d\ln\Gamma/dz \ll -1$, for small z and moderate Γ, but decreases as z increases. Plots of $d\ln\Gamma/dz$ as a function of z for an electron-positron jet are given in the solid curves in Figure 7. For a very large bulk Lorentz factor, the deceleration efficiency decreases significantly because scattering is in the KN regime. For example, we have a much smaller $d\ln\Gamma/dz$ for $\Gamma = 10^5$, as shown in Figure 7.

In the Thomson limit, we can solve (2.1) with (2.8) to find

$$\Gamma(z) \approx \frac{\Gamma_0}{1+\eta\Gamma_0\xi_T}, \tag{3.2}$$

where Γ_0 is the initial value at $z = z_0$, and

$$\xi_T(z_0,z) = \tfrac{1}{15}\mu_p\frac{R_g}{z_0}\left(\frac{R_0}{z_0}\right)^5\left(1-\frac{z_0^5}{z^5}\right)\frac{\langle\gamma^2\rangle}{\langle\gamma\rangle}. \tag{3.3}$$

For $p = 3$ and the distribution given by (2.7), ξ_T reduces to

$$\xi_T \approx 10^2\frac{R_g}{z_0}\left(\frac{R_0}{z_0}\right)^5\left(1-\frac{z_0^5}{z^5}\right)\gamma_{\min}\ln(\gamma_{\max}/\gamma_{\min}). \tag{3.4}$$

Assuming that the initial value of Γ is large and

$\eta\Gamma_0\,\xi_T \gg 1$,

one has the asymptotic value given by

$$\Gamma(\infty) \approx \frac{1}{\eta\,\xi_T(z_0,\infty)}. \tag{3.5}$$

For, $p = 3$, $\gamma_{\max}/\gamma_{\min} = 5\times10^3$, $\gamma_{\min} = 50$, $R_{\min} = 2R_g$, and $z_0 = 10R_g$, even with $\Gamma_0 \gg 1$, we have $\Gamma(\infty) \approx 1$ for $\eta = 0.1$, and $\Gamma(\infty) \approx 10$ for $\eta = 0.01$. Thus, in the Thomson limit, radiation drag is indeed a severe constraint on Γ as already shown in earlier work, e.g. by Melia & Königl (1989), Sikora et al. (1996).

Deceleration described by (3.2) applies only for small Γ or $\gamma_{\max}$. When Γ satisfies (2.16), deceleration is mainly due

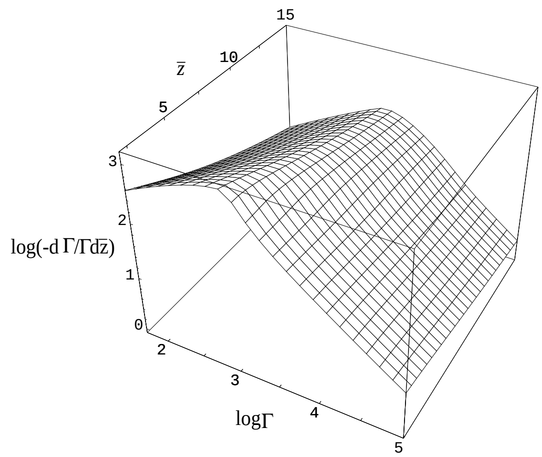

Figure 6. A plot of $-d\ln\Gamma/d\bar{z}$ vs. $\bar{z}$ (with $\bar{z} = z/R_g$) and Γ. The disc parameters are the same as in Figure 5.

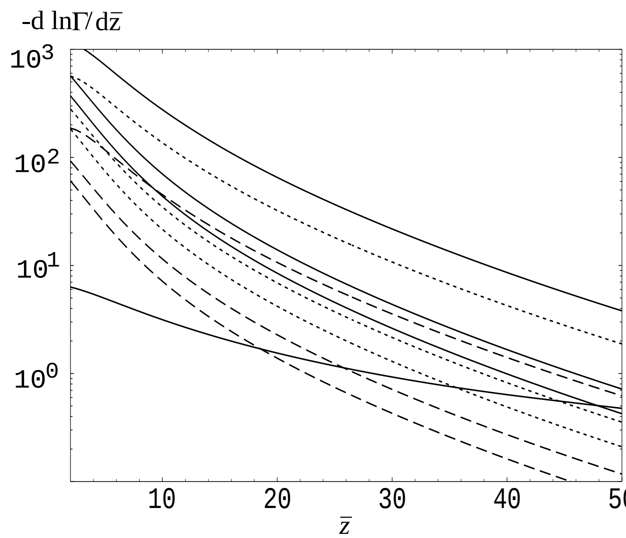

Figure 7. Plots of $-d\ln\Gamma/d\bar{z}$ vs. $\bar{z}$ ($\bar{z} = z/R_g$). The solid curves, from bottom to top corresponding to $\Gamma = 10^5$, 50, 10^2, 10^3, are for a pure electron-positron jet (i.e. $n_p/n_{e0} = 0$, cf. Eq. 3.1). The dotted and dashed curves are for the jet containing cold protons with $n_p/n_{e0} = 0.1$ and 0.5, respectively (cf. Sec. 3.2). In each of these two cases, the curves from bottom to top correspond to $\Gamma = 50$, 10^2, 10^3. The disc parameters are the same as in Figure 5.

to particles scattering in the KN regime. From (2.17), and using (2.1), the bulk Lorentz factor is calculated to be

$$\Gamma(z) \approx \frac{\Gamma_0}{[1+\eta\Gamma_0^{(p-2)}\xi_{\rm KN}]^{1/(p-2)}}, \tag{3.6}$$

with

$$\xi_{\rm KN} = \frac{3\alpha(p-2)^2\mu_p\tilde{\varepsilon}_R^{p-3}}{16\pi 2^{p-1}(2p-1)}\frac{R_g}{R_0}\left(\frac{R_0}{z_0}\right)^{2p-1}\left[1-\left(\frac{z_0}{z}\right)^{2p-1}\right]\gamma_{\min}^{p-2}, \tag{3.7}$$

where $p > 2$, $\alpha = 4.4 - 2.6$, $\tilde{\varepsilon}_R = 5\times10^{-5}$. Deceleration is significantly slower than that calculated from the force in the Thomson approximation since $\xi_{\rm KN}$ is smaller than $\xi_{\rm T}$ by a factor of $5\gamma_{\min}\ln(\gamma_{\max}/\gamma_{\min})$ (for $p = 3$). Eq. (3.6) applies only within a narrow range of Γ (i.e. $1/\langle\gamma\rangle \le \varepsilon_R \le 1/\gamma_{\min}$) as shown in Figure 5.

For even larger Γ_0, the drag is mainly due to scattering in the KN regime (2.18). Retaining only the first term on the right hand side of (2.18), we have

$$\Gamma(z) = \Gamma_0 - \frac{3\eta\mu_p}{16\pi\langle\gamma\rangle\tilde{\varepsilon}_R^2}\,\frac{R_g}{z_0}\left(1-\frac{z_0}{z}\right), \tag{3.8}$$

for $z_0 \le z \le z_1$, where z_1 is the distance at which $\Gamma(z_1)$ is so small that (3.8) does not apply. Figure 8 shows the rapid drop of $\Gamma(z)$ with the distance z, where we assume that the jet starts with $\Gamma_0 = 10^5$ at $z_0 = 5R_g$ and $10R_g$, respectively. In each case, the first curve from the left corresponds to the deceleration of an $e^{\pm}$ jet. The solid curves correspond to deceleration in the Thomson regime, and are calculated using (2.6). The bulk Lorentz factor decreases from $\Gamma = 10^5$ to $\Gamma = 10^3$ within a distance $\Delta z \ll z_0$. Radiation drag is effective except for $\Gamma_0 \ge (3\eta\mu_p/16\pi\langle\gamma\rangle\tilde{\varepsilon}_R^2)(R_g/z_0) \approx 5\times 10^6(\eta/0.1)(R_g/z_0)$ (for $\langle\gamma\rangle = 100$). However, for such a large Γ_0, the second term becomes important, and Γ decreases exponentially according to

$$\ln(\Gamma/\Gamma_0) \approx \\ -\frac{3\eta\mu_p(p-1)}{4\pi p}\int_{z_0}^{z} dz'\,\frac{R_g}{z'^2}\,\frac{1-\cos\tilde{\theta}_R}{\tilde{\varepsilon}_R\langle\gamma\rangle\gamma_{\min}}\ln(2\varepsilon_R\gamma_{\min}). \tag{3.9}$$

For $p = 3$, we have

$$\ln(\Gamma/\Gamma_0) \approx -5.3\left(\frac{\eta}{0.1}\right)\frac{R_g R_0^2}{z_0^3}\left(1-\frac{z_0^3}{z^3}\right)\frac{\ln(2\varepsilon_R\gamma_{\min})}{\tilde{\varepsilon}_R\gamma_{\min}^2}, \tag{3.10}$$

with $\varepsilon_R = \Gamma_0\tilde{\varepsilon}_R$. The drag strongly depends on $\gamma_{\min}$, and can be reduced for large $\gamma_{\min}$.

3.2 A jet containing protons

If a jet is heavily loaded with protons, the effect of radiation drag is reduced significantly, since protons scatter photons with much a smaller cross section compared to electrons, and the presence of protons effectively increases the inertia. When the jet contains cold protons, the energy density is $E = 2n_{e0}\gamma_{\min} + n_p\mu_p$ where n_p is the number density of protons and the electron spectral index is assumed to be $p = 3$ (cf. Eq. 2.7). Suppose that n_p is so large that the condition

$$\delta \equiv \frac{\mu_p n_p}{2\gamma_{\min} n_{e0}} > 1 \tag{3.11}$$

is satisfied. The value δ in Eq. 3.11, corresponding to the ratio of the cold proton energy density to the electron energy density, can increase significantly if protons are relativistic in the jet frame. Then, f_z/E is reduced by a factor δ. The asymptotic $\Gamma(\infty)$ given by (3.5) would increase by a factor δ. For example, for $\gamma_{\min} = 50$, one must include the inertia of protons if $n_p/n_{e0} > 0.05$, and the drag force would be significantly reduced.

The effect of protons on the deceleration efficiency is shown in Figure 7 by dotted curves for $n_p/n_{e0} = 0.1$ and dashed curves for $n_p/n_{e0} = 0.5$. We have smaller $d\ln\Gamma/dz$ than that for the $e^{\pm}$ jet, indicating a decrease in the deceleration efficiency. A relatively weaker radiation drag on jet containing protons can also be seen in Figure 8. The jets with $n_p/n_{e0} = 0.1$ and 0.5 have much higher terminal Lorentz factors than the pure $e^{\pm}$ jet.

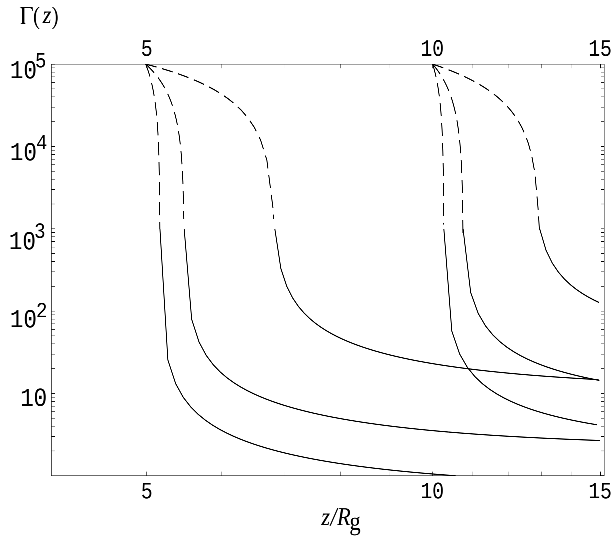

Figure 8. Deceleration of jets. Deceleration in the KN regime and Thomson regime are indicated respectively by dashed and solid part of the curves. The jet is assumed to start with $\Gamma = 10^5$ at $z = 5R_g$ and $z = 10R_g$. In each case, the curves from left to right correspond to $n_p/n_{e0} = 0$ (a pure electron-positron jet), $n_p/n_{e0} = 0.1$, and $n_p/n_{e0} = 0.5$. The efficiency of disc emission, $\eta = 0.05$, is used. Protons are assumed to be cold.

3.3 Energy loss due to inverse Compton scattering

In the calculation of the radiation force, we assume that the plasma in the jet is highly relativistic. In practice, the particle distribution is determined by the various energy loss processes and the injection rate of high energy particles. The energy loss rate due to inverse Compton scattering can be derived from $-\dot{\gamma} = -\beta\cdot d\mathbf{p}/dt$ with $d\mathbf{p}/dt$ given by (2.5). In the Thomson limit, the loss rate is obtained in the jet frame (K_j) as

$$\begin{aligned}-\langle\dot{\gamma}\rangle_a =& \int_{R_{\min}}^{R_{\max}} dR\,\frac{RF(R)}{R^2+z^2}\,\Gamma^2\,(1-\beta_b\cos\tilde{\theta}_R)^2\,\frac{4\sigma_T}{3}\gamma^2\tilde{\varepsilon}_R \\ &\approx \tfrac{2}{3}\mu_p\eta\frac{cR_g}{z^2}\left(\frac{R_0}{z}\right)^4\Gamma^2\gamma^2,\end{aligned} \tag{3.12}$$

where $\langle\ldots\rangle_a$ represents an average over Ω_e, and the approximation is valid only for $\Gamma \gg z/R_0$. In the large angle approximation, we have $-\langle\dot{\gamma}\rangle_a \propto \gamma^2\Gamma^2$. In the small angle approximation $\tilde{\theta}_R \ll \Gamma^{-1}$, i.e. the photon field is from a point source, we have $-\langle\dot{\gamma}\rangle_a \propto \gamma^2/\Gamma^2$. From (3.12), the time scale in K for energy loss for $\Gamma\gamma < 1/\tilde{\varepsilon}_R$ and $z > R_0$ is estimated to be

$$\begin{aligned}t_{\rm IC} &\approx \tfrac{3}{2}\frac{z^2}{cR_g}\left(\frac{z}{R_0}\right)^4\frac{1}{\Gamma\gamma\eta} \\ &= 0.017\,{\rm s}\left(\frac{0.1}{\eta}\right)\left(\frac{\tilde{\varepsilon}_R}{6\times10^{-5}}\right)\left(\frac{1/\tilde{\varepsilon}_R}{\Gamma\gamma}\right)\left(\frac{z}{10R_g}\right)^6,\end{aligned} \tag{3.13}$$

where $\tilde{\varepsilon}_R = 6\times10^{-5}$ corresponds to 30 eV photons. For $\Gamma\gamma \ge 1/\tilde{\varepsilon}_R$, the time scale should be calculated in the KN limit.

In the KN scattering regime, their energy loss rate is much slower, i.e.

$$
\begin{aligned}
-\langle\dot{\gamma}\rangle_a &\approx \int_{R_{\min}}^{R_{\max}} dR\, \frac{RF(R)}{R^2+z^2}\, \frac{3\sigma_T}{8\tilde{\varepsilon}_R} \ln(2\sqrt{e}\gamma\varepsilon_R) \\
&\approx \tfrac{3}{4}\, \frac{\mu_p\eta}{\tilde{\varepsilon}_R^2}\, \frac{cR_g}{z^2} \ln(2\sqrt{e}\gamma\Gamma\tilde{\varepsilon}_R).
\end{aligned}
\tag{3.14}
$$

Unlike (3.12) in the Thomson limit, the energy loss rate increases only slowly with increasing Γ and γ. In K, the characteristic time for the energy loss is

$$
t_{\rm KN} \approx 0.03\,{\rm s}\left(\frac{0.1}{\eta}\right)\left(\frac{\tilde{\varepsilon}_R}{6\times10^{-5}}\right)\left(\frac{z}{10R_g}\right)^2 \frac{\Gamma\gamma\tilde{\varepsilon}_R}{\ln(3.3\Gamma\gamma\tilde{\varepsilon}_R)}, \tag{3.15}
$$

where $\Gamma\gamma\tilde{\varepsilon}_R \geq 1$.

Plasmas in the jet are likely to be magnetized. Then, particles would also radiate synchrotron emission. The energy loss rate due to synchrotron emission is given by

$$
\frac{d\gamma}{dt} \approx \frac{1}{4\pi}\frac{\sigma_{\rm T}B^2\gamma^2}{m_e c}, \tag{3.16}
$$

where B is the magnetic field in the jet frame. Thus, the synchrotron time scale is

$$
t_s \approx 3\times10^3\,{\rm s}\left(\frac{10\,{\rm G}}{B}\right)^2\left(\frac{10^2}{\gamma}\right). \tag{3.17}
$$

The energy loss due to synchrotron emission can be comparable to (3.13) and (3.15) only for strong magnetic fields or large γ.

Because of the short time scales indicated by (3.13) and (3.15) near the black hole, for plasmas in the cell to be highly relativistic one needs an efficient injection of electron positron pairs, e.g. through cascades or acceleration. The relevant processes, either pair cascades or direct acceleration of electrons (positrons), must be fast enough to overcome energy loss due to inverse Compton scattering or synchrotron radiation. Although details of acceleration near a black hole are not well understood, the existence of a rapid acceleration mechanism that is able to accelerate particles to ultrarelativistic energies within a short time scale cannot be ruled out. One possibility is acceleration by a rotation-induced potential drop, similar to that occuring in pulsars, where particles extracted from the neutron star are accelerated to ultrarelativistic energies within a much shorter time scale than the rotation period (e.g. Michel 1987). Particles injected at radial distance $R_{\rm inj}$ to the black hole are acclerated to energy $\gamma \approx \sigma^{2/3}\Delta R/R_{\rm inj}$ after travelling a distance ΔR, where $\sigma = e\Delta\Phi/m_e c^2$, $\Delta\Phi$ is the potential drop which can be estimated from the total power output, L_0, of the AGN, and $\Delta R/R_{\rm inj} \ll 1$ (e.g. Michel 1987). Then, the acceleration time $t_{\rm acc} = \Delta R/c$ is estimated to be

$$
t_{\rm acc} = \frac{\gamma R_{\rm inj}}{c\sigma^{2/3}} \approx 10^{-3}\,{\rm s}\left(\frac{\gamma}{10^4}\right)\left(\frac{R_{\rm inj}}{2R_g}\right), \tag{3.18}
$$

where $\sigma^{2/3} \approx 10^{10}$ for $L_0 = 10^{46}\,{\rm erg\,s^{-1}}$. Since $t_{\rm acc} < t_{\rm IC}$, $t_{\rm KN}$, electrons (positrons) can be accelerated to the energies in the KN regime.

For magnetized plasmas, the condition for relativistic plasmas to be contained in the jet requires that the gyroradius being less than the characteristic transverse size, R_j, of the jet. Since the gyroradius is given by $\rho_g = 2\times10^7\,{\rm cm}\,(\gamma/10^4)(1\,{\rm G}/B)$ where B is the magnetic field, for the characteristic transverse size of the jet, $R_j \approx R_g = 1.5\times10^{13}\,{\rm m}\,(M/10^8M_\odot)$, the condition $\rho_g < R_j$ should be easily satisfied. It can also be shown that the approximation made earlier (Eq. 2.5), i.e. neglecting electron gyration, is valid. The cyclotron time scale $t_c \approx \rho_g/c \approx 10^{-3}\,{\rm s}\,(\gamma/10^4)(1\,{\rm G}/B)$, is much shorter than $t_{\rm IC}$, $t_{\rm KN}$, t_s, and even much shorter than the characteristic time of deceleration, which is typically $> 1\,{\rm s}$.

4 CONCLUSIONS AND DISCUSSION

Radiative deceleration of relativistic jets due to inverse Compton scattering is discussed in both the Thomson and KN scattering regimes. We show that KN scattering is important in deceleration of ultrarelativistic jets with initial bulk Lorentz $\Gamma > 10^3$. For $\Gamma \gg 1$, near the black hole and in the jet frame, the incoming photons are beamed towards the hole, and so the main contribution to the drag of the jet is from head-on scattering by forward moving particles. These particles are more likely to be in the KN regime as they see photons of the highest energy ($\varepsilon' > 1$). Particles scattering in the Thomson regime may contribute positively to the radiation force but overall KN scattering is dominant and results in deceleration. Thus, scattering in the KN regime should be included in calculations of the radiation force when $\Gamma > 10^3$. Our result shows that in the KN regime, radiation drag is reduced, but still severely constrains the speed of the jet bulk flow. Thus, Compton drag can decelerate an $e^\pm$ jet starting with *any* $\Gamma > 10$ in the region sufficiently close to the black hole down to the value $\Gamma < 10$. The efficiency of deceleration is significantly reduced if the jet contains protons since protons have much smaller scattering cross section and the effect of protons is to increase the inertia of the jet.

According to the unified scheme (e.g. Urry & Padovani 1995), blazars are radio-loud quasars, and if this is true, a relativistic jet with sufficient particle kinetic luminosity is required to power radio lobes at a larger distance. The results given here show that because of radiation drag the ability of an electron-positron jet to power large scale radio lobes is severely constrained. For example, consider an $e^\pm$ jet with an initial luminosity $\dot{N}_i\Gamma_i \approx L_d$, where $\dot{N}_i$ and $\Gamma_i \gg 1$ are the initial particle flux and Lorentz factor. As a result of Compton drag, the flow slows down to $\Gamma_f < 10$ with most of the energy going into radiation. Thus, even with pair cascades $\dot{N}_f \gg \dot{N}_i$, we may still have $\dot{N}_f\Gamma_f \ll \dot{N}_i\Gamma_i$. The constraint can be overcome if $e^\pm$ are re-accelerated at a distance further away from the central region or if there is outflow of accelerated protons as suggested in a two-flow model by Sol, Pelletier & Asseo (1989). In their model, radio lobes are powered by outflow of p-e plasma jets and $e^\pm$ jets are dominant only in the subparsec region.

In our discussion, the external soft photons are assumed to come only from the disc emission which is the sum of blackbody emission from series of rings centred at the black hole, and is similar to the model discussed by Demer & Schlickeiser (1993). Generalization of the calculation to include other radiation fields, such as that due to a disc torus (Protheroe & Biermann 1997), and reprocessed radiation, should be straightforward. The effect on the jet due to scattering of photons from the broad-line region may also be important, and is not considered here. In calculating the average force, we assumed an isotropic (angular) distribution of electrons (or positrons) with a power law. Some mechanism, e.g. pitch angle scattering, is required for isotropization since inverse Compton scattering itself tends to make the distribution anisotropic.

ACKNOWLEDGEMENTS

QL acknowledges the receipt of Australian Research Council (ARC) Postdoctoral Fellowship.

REFERENCES

Begelman, M. C., Blandford, R. D. & Rees, M. J. 1980, Nature, 287, 307.

Blandford, R. D. 1990, in Active Galactic Nuclei, eds. R.D. Blandford, H. Netzer & L. Woltjer, (Springer-Verlag, Berlin) p. 161.

Blumenthal, G. R. & Gould, R. J. 1970, Rev. Mod. Phys., 42, 237.

Dermer, C. D. & Schlickeiser, R. 1993, ApJ, 416, 458.

Eracleous, M., Livio, M., Halpern, J. P. & Storchi-Bergmann, T. 1995, ApJ, 438, 610.

Gaidos, J. A. et al. 1996, Nature, 383, 319.

Haswell, C. A., Tajima, T. & Sakai, J. I. 1992. 401, 495.

Königl, A. 1994, in The First Stromlo Symposium: The Physics of Active Galaxies, ed. G.V. Bicknell, M.A. Dopita & P.J. Quinn, ASP Conf. Series Vol. 54, p. 33.

Luo, Q. 1998, in preparation.

Melia, F. & Königl, A. 1989, ApJ, 340, 162.

Michel, F. C. 1987, ApJ, 321, 714.

O'Dell, S. L. 1981, ApJ, 243, L147.

Phinney, E. S. 1982, MNRAS, 198, 1109.

Phinney, E. S. 1987, in Zensus, J. A. & Pearson, T. J. eds. Superluminal Radio Sources, (Cambridge Univ. Press), p. 301.

Protheroe, R. J., Biermann, P. L. 1997, Astroparticle Phys., 6, 293.

Quinn, J. et al. 1996, 456, L83.

Reynolds, S. P. 1982, ApJ, 256, 38.

Schubnell, M. S. et al. 1996, ApJ, 460, 644.

Sikora, M. et al. 1996, MNRAS, 280, 781.

Sol, H., Pelletier, G. & Asséo, E. 1989, MNRAS, 237, 411.

Thompson, D. J. et al. 1995, ApJS, 101, 259.

Urry, C. M. & Padovani, P. 1995, PASP, 107, 803.

von Montigny, C. et al. 1995, ApJ, 440, 525.

APPENDIX A: MOMEMTUM TRANSFER DUE TO COMPTON SCATTERING

Calculation of momemtum transfer (2.5) requires the full KN differential cross $d\sigma/d\varepsilon_s d\Omega_s$ which was discussed in details by Blumenthal & Gould (1970). Here, we use the following approximation (in K_j) (Reynolds 1982; Dermer & Schlickeiser 1993)

$$\frac{d\sigma}{d\varepsilon_s d\Omega_s} \approx \sigma_{\rm T}\delta\Big[\varepsilon_s - \gamma^2\varepsilon(1-\beta\cos\Theta)\Big]\,\delta(\Omega_s-\Omega_e), \tag{A1}$$

for the Thomson regime ($\varepsilon' < 1$) and

$$\frac{d\sigma}{d\varepsilon_s d\Omega_s} \approx \frac{3\sigma_{\rm T}}{8\varepsilon'}\ln(2\sqrt{e}\varepsilon')\delta(\varepsilon_s-\gamma)\delta(\Omega_s-\Omega_e), \tag{A2}$$

for the KN regime ($\varepsilon' \geq 1$), where $\sigma_{\rm T}$ is the Thomson cross section, ε' is the incoming photon energy in the electron rest frame, $\cos\Theta = \cos\theta\cos\theta_e + \sin\theta\sin\theta_e\cos(\phi-\phi_e)$, Θ is the angle between the incoming photon direction and the electron motion, the delta function $\delta(\Omega_s-\Omega_e)$ describes the beaming approximation.

To evaluate (2.5), particles with γ can be broadly separated into two groups: one group of particles with $\cos\theta_e < \mu_c$) scatter in the Thomson regime with (A1) and the other group with $\cos\theta_e \geq \mu_c$ scatter in the KN regime with (A2). This approximation is similar to that was used Dermer & Schlickeiser (1993) in calculating scattered photon spectrum. Thus, using (A1) and (A2), the radiation force (2.5) can be written approximately into the form

$$\begin{aligned}
f_z &\equiv \int d\Omega_e d\gamma\,\frac{dp_z}{dt}n_e(\gamma,\Omega_e)\\
&\approx -\sigma_{\rm T}\int dR\,\frac{RF(R)}{2\pi(R^2+z^2)}\\
&\times\tilde{\varepsilon}_R\Gamma^2(1-\beta_b\cos\tilde{\theta}_R)^2\int d\Omega_e d\gamma\,n_e(\gamma,\Omega_e)\\
&\times\Big\{(1-\beta\cos\Theta_R)\Big[\gamma^2(1-\beta\cos\Theta)\cos\theta_e-\cos\theta_R\Big]H(1-\varepsilon'_R)\\
&+\tfrac{3}{8}\frac{\ln(2\sqrt{e}\varepsilon'_R)}{\Gamma\gamma\tilde{\varepsilon}_R}\big(\gamma\cos\theta_e-\varepsilon_R\cos\theta_R\big)H(\varepsilon'_R-1)\Big\},
\end{aligned} \tag{A3}$$

where $H(\varepsilon'_R-1)=1$ for $\varepsilon'_R\geq 1$ and $H(\varepsilon'_R-1)=0$ for $\varepsilon'_R < 1$, $n_e(\gamma,\Omega_e)$ is the particle distribution as defined earlier (Eq. 2.7). The terms with $H(1-\varepsilon'_R)$ and $H(\varepsilon'_R-1)$ correspond respectively to scattering in the Thomson and KN regimes.

Accordingly, f_z is written as a sum of two components, $f_z = f_{z,{\rm T}} + f_{z,{\rm KN}}$ where $f_{z,{\rm T}}$, $f_{z,{\rm KN}}$ describe the contributions to the force from scattering in the Thomson and KN regime, respectively, and they are

$$\begin{aligned}
f_{z,{\rm T}} &= -\sigma_{\rm T}\int dR\,\frac{RF(R)}{2\pi(R^2+z^2)}\tilde{\varepsilon}_R\Gamma^2(1-\beta_b\cos\tilde{\theta}_R)^2\\
&\times\int d\gamma\int\frac{d\phi_e}{2\pi}\int_{-1}^{\mu_c}\frac{d\cos\theta_e}{2}\,n_e(\gamma,\Omega_e)(1-\beta\cos\Theta_R)\\
&\times\Big[\gamma^2(1-\beta\cos\Theta)\cos\theta_e-\cos\theta_R\Big],
\end{aligned} \tag{A4}$$

and

$$\begin{aligned}
f_{z,{\rm KN}} &= -\sigma_{\rm T}\int dR\,\frac{RF(R)}{2\pi(R^2+z^2)}\tilde{\varepsilon}_R\Gamma^2(1-\beta_b\cos\tilde{\theta}_R)^2\\
&\times\int d\gamma\int\frac{d\phi_e}{2\pi}\int_{\mu_c}^{1}\frac{d\cos\theta_e}{2}\,n_e(\gamma,\Omega_e)\tfrac{3}{8}\frac{\ln(2\sqrt{e}\varepsilon'_R)}{\Gamma\gamma\tilde{\varepsilon}_R}\\
&\times\big(\gamma\cos\theta_e-\varepsilon_R\cos\theta_R\big),
\end{aligned} \tag{A5}$$

where μ_c, $n_e(\gamma,\Omega_e)$ are defined by (2.12), (2.7). Integration over $\cos\theta_e$ can be easily done using approximation $|\sin\theta_R| \ll |\cos\theta_R| \approx 1$, $\cos\theta_R \approx -1$. In this approximation, the integrands in (A4) and (A5) can be regarded as independent of ϕ_e. Then, integrating over $\cos\theta_e$, we obtain

$$\begin{aligned}
&f_{z,{\rm T}} =\\
&-\tfrac{1}{2}\sigma_{\rm T}C_0 n_{e0}\int dR\,\frac{RF\tilde{\varepsilon}_R\Gamma^2}{2\pi(R^2+z^2)}(1-\beta_b\cos\tilde{\theta}_R)^2\int d\gamma\,\gamma^{-p}\\
&\times\Big\{\gamma^2\Big[\tfrac{1}{2}(\mu_c^2-1)-\tfrac{2}{3}\beta\cos\theta_R(\mu_c^3+1)+\tfrac{1}{4}(\mu_c^4-1)\Big]\\
&-\cos\theta_R(\mu_c+1)+\tfrac{1}{2}(\mu_c^2-1)\Big\},
\end{aligned} \tag{A6}$$

$$
\begin{aligned}
f_{z,\mathrm{KN}} \approx & -\tfrac{3}{8}\sigma_{\mathrm{T}} C_0 n_{e0} \int dR\, \frac{RF}{2\pi(R^2+z^2)} \frac{1}{4\tilde{\varepsilon}_{R}} \int d\gamma\, \gamma^{-p} \\
& \times \left\{ \left(1-\mu_c^2\right) \ln 2 - \frac{1-\mu_c}{\beta\cos\theta_{R}} \right. \\
& - \frac{2\varepsilon_{R}\cos\theta_{R}}{\gamma} \left[(1-\mu_c)\ln(2/\sqrt{e}) \right. \\
& \left. \left. + \left(1 - \frac{1}{\beta\cos\theta_{R}}\right) \ln(2\varepsilon_{R}\gamma) \right] \right\} H(\gamma\varepsilon_{R} - \tfrac{1}{2}).
\end{aligned} \tag{A7}
$$

Eq. (A6) reduces to Eq. (2.6) or (2.8) by assuming $\mu_c = 1$, i.e. all particles are in the Thomson scattering regime. Let I_{T} and I_{KN} represent γ-integration in (A6) and (A7); I_{T} and I_{KN} are calculated to be

$$
\begin{aligned}
I_{\mathrm{T}} = & \frac{1}{2(p+1)\varepsilon_R^2} \left(1 + \frac{1}{2\varepsilon_R^2}\right) \left(\gamma_c^{-p-1} - \gamma_{\max}^{-p-1}\right) \\
& + \frac{1}{3p\varepsilon_R^3} \left(\gamma_{\max}^{-p} - \gamma_c^{-p}\right) + \frac{4}{3(3-p)} \left(\gamma_c^{3-p} - \gamma_{\min}^{3-p}\right) \\
& + \frac{2}{p-1} \left(\gamma_{\min}^{1-p} - \gamma_c^{1-p}\right),
\end{aligned} \tag{A8}
$$

$$
\begin{aligned}
I_{\mathrm{KN}} = & \frac{2}{p-1} \left(\gamma_c^{1-p} - \gamma_{\max}^{1-p}\right) \\
& + \frac{1}{p} \left[\frac{\ln(4e)}{\varepsilon_R} + 2\varepsilon_R \ln(4/e) + 4\varepsilon_R/p \right] \left(\gamma_c^{-p} - \gamma_{\max}^{-p}\right) \\
& - \frac{1}{p+1} \left[\frac{\ln 2}{\varepsilon_R^2} + \ln(4/e) \right] \left(\gamma_c^{-p-1} - \gamma_{\max}^{-p-1}\right) \\
& + \frac{4\varepsilon_R}{p} \left[\gamma_c^{-p} \ln(2\varepsilon_R\gamma_c) - \gamma_{\max}^{-p} \ln(2\varepsilon_R\gamma_{\max}) \right],
\end{aligned} \tag{A9}
$$

where $\gamma_c = \max\{1/\varepsilon_{R}, \gamma_{\min}\}$. Then, (A6) and (A7) can be further written into the form

$$
f_{z,\mathrm{T}} = - \tfrac{1}{2}\sigma_{\mathrm{T}} C_0 n_{e0} \int_{R_{\min}}^{R_{\max}} dR\, \frac{RF\tilde{\varepsilon}_{R}\Gamma^2(1-\beta_b\cos\tilde{\theta}_{R})^2}{2\pi(R^2+z^2)} I_{\mathrm{T}}, \tag{A10}
$$

$$
f_{z,\mathrm{KN}} \approx -\tfrac{3}{8}\sigma_{\mathrm{T}} C_0 n_{e0} \int_{R_{\min}}^{R_{\max}} dR\, \frac{RF\, I_{\mathrm{KN}}}{2\pi(R^2+z^2)} \frac{1}{4\tilde{\varepsilon}_{R}}. \tag{A11}
$$

This paper has been produced using the Royal Astronomical Society/Blackwell Science TEX macros.